

UDC 548.73:541.6:547.13:546.56

**COMPARISON OF COMPUTATIONAL STUDIES WITH
THE X-RAY CRYSTAL STRUCTURE OF DIRECTLY SYNTHESIZED
BIS(D,L-AMINOBUTYRIC)COPPER(II) COMPLEX****R. Kumar, S. Obrai**

Department of Chemistry Dr. B.R. Ambedkar National Institute of Technology, Jalandhar, India
E-mail: rakesh_nitj@yahoo.co.in

Received November, 30, 2012

The important feature of the present work is that the crystal data are obtained first time for the directly synthesized complex $[\text{Cu}(\text{D,L-but})_2]$ from pure zero valent metal and butyric acid in water. Further investigation involves the comparison of structural parameters from the XRD data of the title complex $[\text{Cu}(\text{D,L-but})_2]$ in solid state with the theoretically optimized structure in the gaseous state and its simulated spectra (vibrational and electronic) are generated. The results show that the structural parameters determined by computational studies and crystal structure studies are in good agreement. In the computational calculations, the geometric optimization is carried out using the MM3 method and electronic spectra are calculated using ZINDO, a semi-empirical quantum mechanical method of Scigress explorer 7.7. The theoretical calculations of HOMO—LUMO energies have revealed that the charge transfer interactions occur within the complex. The crystal data for the $[\text{Cu}(\text{D,L-but})_2]$ complex are: space group $P2_1/c$; $a = 11.096(5) \text{ \AA}$, $b = 5.062(4) \text{ \AA}$, $c = 9.475(3) \text{ \AA}$; $\beta = 92.4^\circ$; $\rho_{\text{calcd}} = 1.673 \text{ g/cm}^3$; $Z = 2$.

Keywords: copper metal, direct synthesis, $\text{Cu}(\text{D,L-but})_2$, ZINDO, INDO, HOMO—LUMO.

INTRODUCTION

Coordination compounds based on copper mostly occur in nature and they are the heart of proteins such as blue copper enzymes. The coordination geometry of Cu(II) depends upon the nature and size of the ligands, which describes the wide number of observed complexes for this metal ion and in these complexes coordination number varies from 2 to 7. The stability of these complexes formed between Cu(II) and amino acids (derivatives) makes this transition metal ion suitable for the use in separation techniques, such as chiral ligand exchange chromatography [1]. The direct synthesis of metal complexes starting from zero valent metals is an active area of research both from technological and scientific points of view.

The direct synthesis of coordination compounds possess several advantages over conventional ligand displacement reactions. These include the use of metals as a source of cations, the exclusions of all undesirable ions in the solution, high product purity, and the use of metals which can be purchased at lower cost than their salts [2]. The present study shows that metal complexes can be prepared from the pure metal itself. The crystallographic and computational investigation of the present complex has also been carried out. The molecular mechanics MM3 method of Scigress Explorer 7.7 has been applied for the computational analysis of structural parameters. The semi-empirical quantum mechanical method is used to determine the electronic spectra as well as the HOMO—LUMO energies of the pre-

sent molecule, which shows that charge transfer occurs within the molecule. Molecular mechanics is the application of classical mechanics to molecules [3]. Under this method the positions of the atoms in a molecule, ion, solvate or crystal lattice are determined by forces between the pair of atoms (bonds, van der Waals interactions, hydrogen bonding, and electrostatic interaction). The main aim of molecular mechanics is to adjust the position of the atoms until they find the optimum molecular geometry.

EXPERIMENTAL

The [Cu(D,L-but)₂] complex was synthesized by the reaction with the 1:2 molar ratio of copper metal and (D,L-aminobutyric acid) in an aqueous medium at 70–80 °C for 1–2 h and then left at room temperature. The product was obtained in the form of needle shape blue crystals in the solution. The crystals were decomposed at 260 °C. IR (KBr), cm⁻¹: 3295 s, 3244 s, ν_{as}(NH₂), ν_s(NH₂), 2962 s, 2935 s, ν(C—H), 1615 vs, 1574 vs ν(C=O), 1455 m CH₂-scissor, 1392 s ν(C—O), 877 vs ρ(NH₂), 584 s ν(Cu—N). Copper metal sheets were purified with the help of a sonicator to remove the impurities and then washed with acetone before carrying out the reaction.

XRD data were collected on a Bruker APEX-II CCD diffractometer employing graphite-monochromated MoK_α radiation (λ = 0.71069 Å) at room temperature. The structure was solved [4] by direct methods using SIR-97 program from SHELXTL-PC followed by the full matrix least square refinement with anisotropic thermal parameters for all non-hydrogen atoms [5]. All the hydrogen atoms were attached geometrically, except for those bonded to the amine group. Hydrogen bonding was performed with PARST [6]. The crystal data for the complex are summarized in Table 1.

Table 1

Crystal data and data collection parameters for the [Cu(D,L-but)₂] complex

Empirical formula	C ₈ H ₁₆ CuN ₂ O ₄
Formula weight	267.78
Crystal system	Monoclinic
Crystal size, mm	0.25×0.20×0.10
Color; Shape	Blue; Needle
Space group	<i>P</i> 2 ₁ / <i>c</i>
Unit cell dimensions <i>a</i> , <i>b</i> , <i>c</i> , Å; α, β, γ, deg.	11.096(5), 5.062(4), 9.475(3); 90.00(0), 92.416(5), 90.00(0)
Volume, Å ³ ; <i>Z</i>	531.7(5); 2
ρ _{calc} , g·cm ⁻³	1.673
μ, cm ⁻¹	2.050
<i>F</i> (000)	278.0
Type of data collection	θ—2θ
Range of data collection, deg.	1.84 to 28.28
Limiting frequency	-14 < <i>h</i> < 14, -6 < <i>k</i> < 6, -12 < <i>l</i> < 12
Total / Independent reflections	7153 / 1320 [<i>R</i> (int) = 0.0328]
Completeness to θ = 28.28 %	99.8
Refinement method	Full matrix least squares on <i>F</i> ²
Goodness-of-fit on <i>F</i> ²	1.209
Final <i>R</i> indices [<i>I</i> > 2σ(<i>I</i>)]	<i>R</i> 1 = 0.0396, <i>wR</i> 2 = 0.0977
<i>R</i> indices (all data)	<i>R</i> 1 = 0.0552, <i>wR</i> 2 = 0.1205
Largest diff. peak & hole, e/Å ³	0.759 and -0.829

Fig. 1. ORTEP drawing of the complex showing the atom labeling scheme

RESULTS AND DISCUSSION

The final X-ray crystal structure is shown in Fig. 1. The coordination number around the Cu^{2+} ion is four resulting in square-planar geometry. Copper(II) is bonded with the carboxylate oxygen atom O1, symmetry related O1', the amine nitrogen atom N1, and symmetry related N1' of α -aminobutic acid.

In the title complex, Cu—N distance is 1.986 Å, whereas the Cu—O bond length is 1.942 Å. The structural features of the complex (fractional atomic coordinates and thermal parameters) and possible hydrogen bonding distances are given in Tables 2 and 3.

In the $[\text{Cu}(\text{D,L-but})_2]$ complex, two main well defined hydrophobic and hydrophilic regions are present. The hydrophobic region is formed from the nonpolar side chain of the ethyl group whereas the hydrophilic region contains the Cu(II) ion as well as the carboxylate and amine groups, as is already reported in the literature [11–16].

Table 3 shows the important hydrogen bonds. The molecular structure (Fig. 2) shows the H-bonding interactions involving amine hydrogen and carboxylate oxygen atoms coordinated to Cu(II). The amine nitrogen atom N1 is acting as a double donor of the hydrogen bond through its two hydrogen atoms towards coordinated carboxylate oxygen acting as an acceptor of H-bonds. The amine nitrogen atom N1 also donates its hydrogen bonds to symmetry related O1' of the carboxylate oxygen of the other amino acid group.

COMPUTATIONAL DETAILS

The first step in the computational work is to determine the optimized geometry by energy minimization. The molecular structure (Fig. 3) of the title compound was computed using the MM3 method of molecular mechanics in the gaseous phase. Electronic transitions and vibrational frequen-

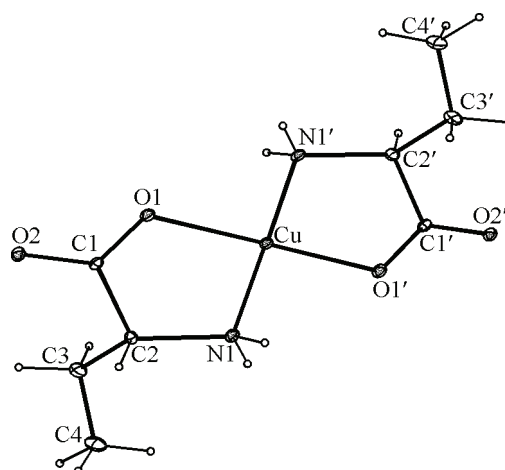


Table 2

Final positional parameters ($\times 10^4$) and equivalent isotropic displacement parameters ($\text{\AA}^2 \times 10^3$) for all atoms in the complex

Atom	x	y	z	U(eq)	Atom	x	y	z	U(eq)
Cu	10000	10000	10000	27(1)	C(1)	8677(2)	8899(5)	7550(3)	25(1)
O(1)	9535(2)	7935(3)	8338(2)	25(1)	C(2)	8023(2)	11336(5)	8117(3)	27(1)
O(2)	8343(2)	7980(4)	6393(2)	36(1)	C(3)	6813(3)	10509(7)	8669(5)	42(1)
N(1)	8796(2)	12582(4)	9229(2)	24(1)	C(4)	6015(4)	12845(9)	9002(6)	64(1)

Table 3

Selected hydrogen bonding distances (Å) and angles (deg.) for the complex

Donor (D)	Hydrogen (H)	Acceptor (A)	D—H...A	D...A	H...A	D...H
N1	H1	O1	151.55(3)	2.964(4)	2.173(3)	.866(3)
N1	H1	O1'	122.03(3)	3.123(3)	2.576(3)	.866(3)
N1	H2	O1	86.40(3)	2.908(3)	2.855(3)	.760(3)

Equivalent position: (') $-x+2, +y+1/2, -z+1/2+1$.

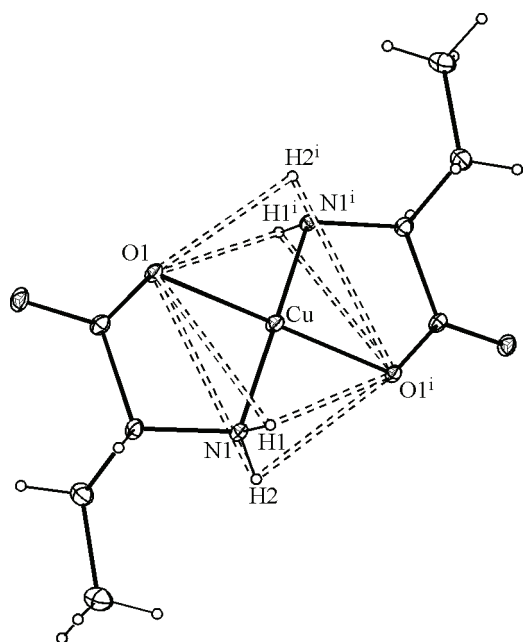


Fig. 2. Molecular structure of the complex showing hydrogen bonding interactions

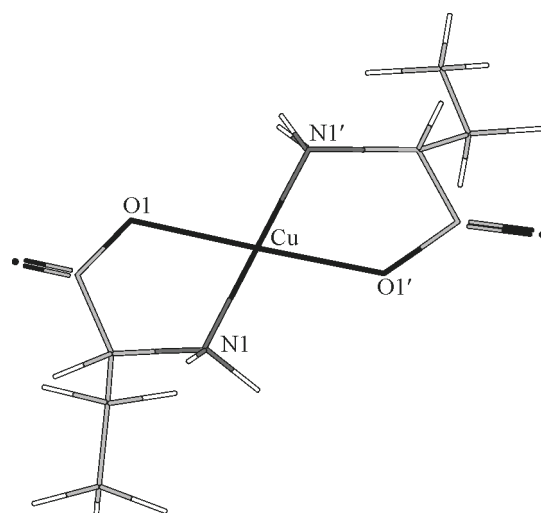


Fig. 3. Optimized geometry of $[\text{Cu}(\text{D,L-but})_2]$

cies of the optimized geometry were computed by quantum mechanics. The electronic properties such as the HOMO—LUMO energies and absorption wavelength were calculated by ZINDO (Zerner's Intermediate Neglect of Differential Overlap program) that computes semi-empirical quantum mechanical values for the properties and spectra of molecules. It is a development of the INDO (Intermediate Neglect of differential Overlap) method and sometimes called INDO/S used for calculating the excited states and electronic spectra of the complex [7].

All the computations were performed [8] with Scigress Explorer 7.7 that includes MM2 and MM3 force fields, which enables minimization calculations for square planar, trigonal bipyramidal, and octahedral geometries [9, 10]. Structural parameters (bond length and bond angles) obtained from XRD and computational methods are in good agreement (Tables 4). Maximum bond length and bond angle deviations for the complex are 0.064 \AA and 1.03° . Simulated vibrational and experimental FT-IR spectra are shown in Fig. 4. The assignment of frequencies of the functional groups is given in Table 5 and it is in good agreement with each other.

Table 4

Comparison of bond lengths (\AA) and bond angles (deg.) from the X-ray data and computational calculations

Bond lengths	Experimental	Theoretical	Deviation	Bond angles	Experimental	Theoretical	Deviation
Cu—N(1)	1.986(2)	2.008	-0.022	O1—Cu—N1	84.50(9)	84.29	0.21
Cu—O(1)	1.942(18)	1.970	-0.028	O1—Cu—N1'	95.50(9)	95.54	-0.04
Cu—N(1')	1.986(2)	1.956	0.03	N1—Cu—O1'	95.50(9)	95.92	-0.42
Cu—O(1')	1.942(18)	2.006	-0.064	O1—Cu—O1'	179.99(1)	178.96	1.03
C(1)—O(1)	1.281(3)	1.362	-0.081	Cu—N1—C2	110.11(16)	110.14	-0.03
C(1)—O(2)	1.233(3)	1.223	0.01	C1—O1—Cu	115.67(16)	118.83	-3.16
C(1)—C(2)	1.540(4)	1.540	0	O2—C1—O1	124.2(2)	121.14	-3.06
C(2)—N(1)	1.473(3)	1.575	-0.102	O1—C1—C2	116.8(2)	113.24	3.56
				O2—C1—C2	119.0(2)	125.29	-6.29
				N1—C2—C3	111.6(3)	119.64	-8.04
				C1—C2—N1	108.9(2)	111.71	-2.80

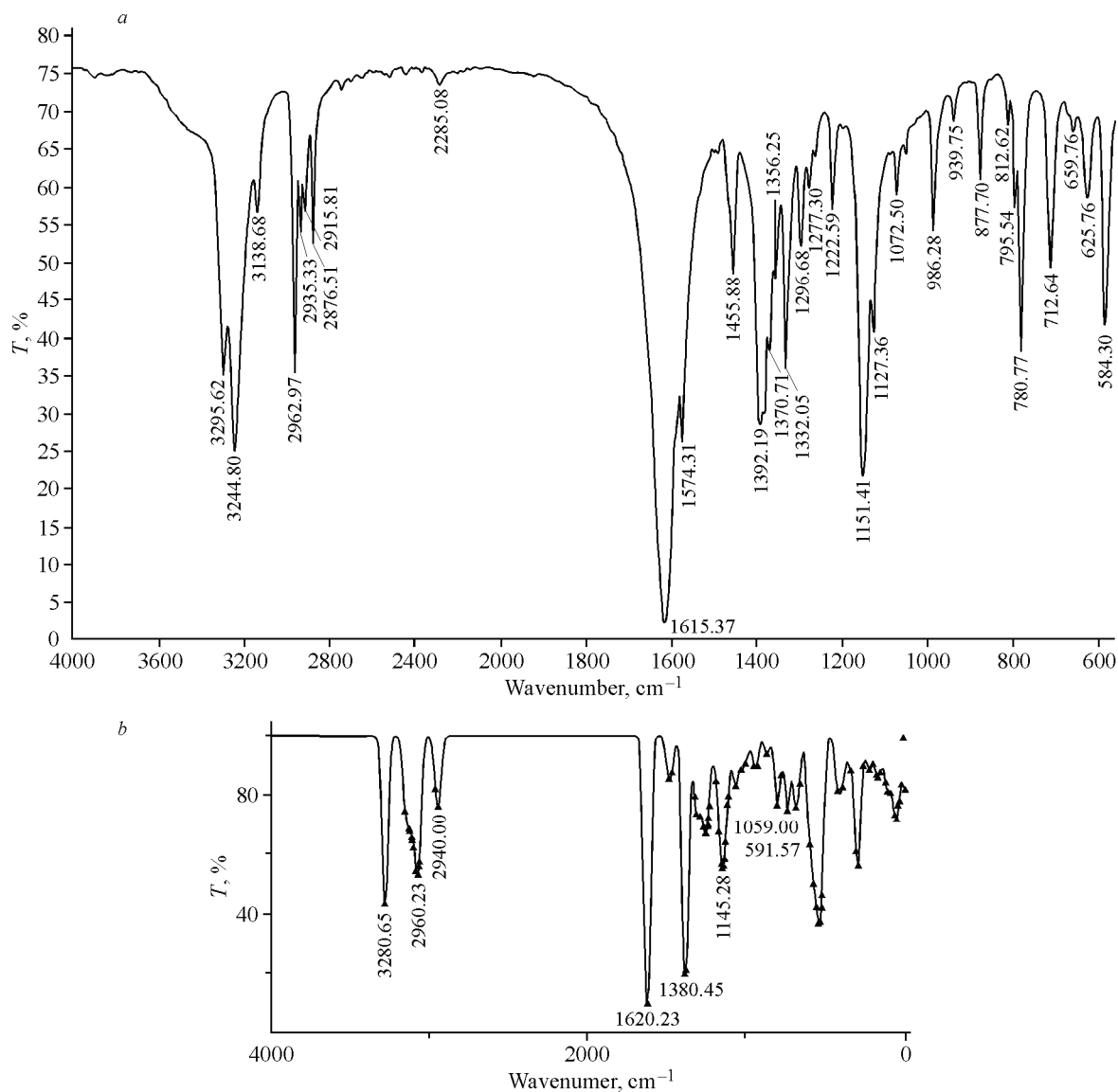


Fig. 4. Experimental (a) and simulated (b) IR spectrum of the $[\text{Cu}(\text{D,L-but})_2]$ complex

Table 5

Comparison of the experimental and simulated vibrational spectra of $[\text{Cu}(\text{D,L-but})_2]$

Infrared (v/cm^{-1}) Experimental	Infrared (v/cm^{-1}) Theoretical	Assignment	Infrared (v/cm^{-1}) Experimental	Infrared (v/cm^{-1}) Theoretical	Assignment
3295 s, 3244 s	3280	$\nu_{\text{as}}(\text{NH}_2)$, $\nu_{\text{s}}(\text{NH}_2)$	1356 m	—	$\nu(\text{C}-\text{CO}_2)$
2962 s	2960	$\nu(\text{C}-\text{H})$	1151s	1145	$\rho(\text{NH}_3^+)$
2935 s	2940	$\nu(\text{C}-\text{H})$	1072 s	1059	$\nu(\text{C}-\text{N})$
1615 vs, 1574 vs	1620	$\nu(\text{C}=\text{O})$	986s	—	$\nu(\text{C}-\text{C})$
1455 m	—	CH_2 -scissor	877vs	—	$\rho(\text{NH}_2)$
1392 s	1380	$\nu(\text{C}-\text{O})$	584s	591	$\nu(\text{Cu}-\text{N})$

vs: very strong; s: strong; m: medium; w: weak.

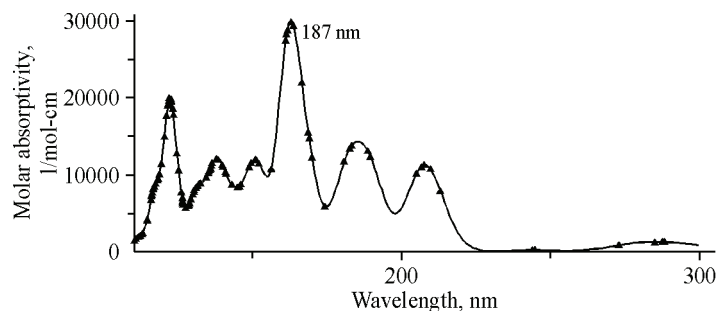


Fig. 5. Simulated UV-visible spectra of the complex

The simulated UV-Vis spectrum is generated by ZINDO and is created due to the electronic transition between molecular orbitals as electromagnetic radiation in the visible and ultraviolet regions absorbed by the molecule. The maximum wavelength for the present complex has been found to be 187 nm (Fig. 5), which corresponds to the HOMO—LUMO electronic transition. In charge transfer transitions, electrons from the ligand-based molecular orbitals are excited into the half-occupied dx^2-y^2 orbital leading to ligand-to-metal charge transfer transitions (LMCT). These transitions are highly intense relative to $d-d$ transitions. Charge transfer transitions generally lie in the UV region, but in the case of metal in high oxidation states, they shift towards the visible region. The charge transfer transitions are key to understand the nature of ligand-metal bonds because high covalency is associated with low energy and intense charge transfer transitions [17]. The intensities of these transitions are proportional to the overlap of the donor and acceptor orbitals involved in the charge transfer process [18]. The HOMO—LUMO energies are -7.373 eV and -0.619 eV whereas the energy gap value is 6.754 eV, as shown in Fig. 6. In the present complex, LMCTs occur in which an electron moves from the HOMO orbital of mainly ligand in character to LUMO that is mainly metal in character.

The HOMO is the orbital that primarily acts as an electron donor and the LUMO is the orbital that largely acts as the electron acceptor, and the gap between the HOMO and LUMO characterizes the molecular chemical stability. The energy gap between the HOMO and LUMO molecular orbitals is a critical parameter in determining the molecular electrical transport properties because it is a measure of electron conductivity. The HOMO—LUMO energy gap could be regarded as a quantitative index in evaluating the impact sensitivity of energetic complexes with similar geometric structures. The less the energy gap is, the more sensitive the energetic complex is. This is in good agreement with the fact that the metallic complex can be used as an initiator due to its high sensitivity [19, 20].

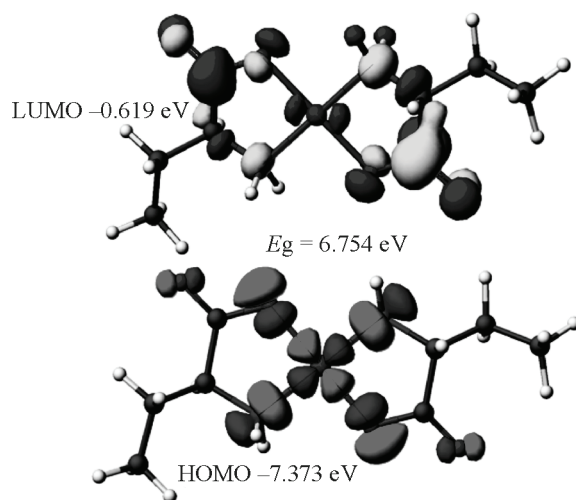


Fig. 6. Molecular orbital surfaces for HOMO and LUMO of $[\text{Cu}(\text{D,L-but})_2]$

CONCLUSIONS

In the present paper, an attempt has been made to prepare the coordination complex from the zero valent metal and to analyze its crystal structure and compare the structural parameters obtained by XRD with the computed data. An attempt has also been made to investigate the simulated spectra (vibrational and electronic spectra) and compare the results of the vibrational spectra with the experimental FT-IR spectra. Again we were successful in getting the results in good agreement. Intense charge transfer transitions are displayed by the simulated electronic spectrum of the complex mainly in the ultra-violet region that shows a good orbital overlap between the ligand (HOMO) and metal (LUMO) orbitals that are important parameters for the chemical reaction. A lower value of the HOMO and LUMO energy gap explains the eventual charge transfer interactions taking place within the molecule.

Acknowledgements. The authors are highly grateful to MHRD, New Delhi for providing research assistantship to Mr. Rakesh Kumar, one of the authors, and Dr. B.R. Ambedkar National Institute of Technology, Jalandhar for providing research infrastructure.

Supplementary data. Crystallographic data for the structure reported in this paper have been deposited with the Cambridge Crystallographic Data Centre as the supplementary publication no. CCDC 878576. This data can be obtained free of charge via <http://www.ccdc.cam.ac.uk/conts/retrieving.html>, or from the Cambridge Crystallographic Data Centre, 12 Union Road, Cambridge CB2 1Ez, UK; fax(+44) 1223-336-033; or e-mail:deposit@ccdc.cam.ac.uk.

REFERENCES

1. *de Bruin T.J.M., Marcelis A.T.M., Zuilhof H. et al.* // Phys. Chem. Chem. Phys. – 1999. – **1**. – P. 4157 – 4163.
2. *Garnovskii A.D., Kharisov B.I., Gojon-Zorrilla G. et al.* // Russ. Chem. Rev. – 1995. – **64**. – P. 201 – 221.
3. *Comba P., Hambley T.W.* Molecular Modeling of Inorganic Compounds. – Weinheim: Wiley-VCH, 2001.
4. *Altomare A., Burla M.C., Camalli M. et al.* // J. Appl. Crystallogr. – 1999. – **32**. – P. 115 – 119.
5. *Sheldrick G.M.* SHELX97, Release 97-2. – University of Göttingen, Germany, 1997.
6. (a) *Nardelli M.* // Comput. Chem. – 1983. – **7**. – P. 95 – 97. (b) *Nardelli M.* // J. Appl. Crystallogr. – 1995. – **28**. – P. 659.
7. *Zerner M.* Reviews in Computational Chemistry / K.B. Lipkowitz and D.B. Boyd. – New York: VCH Publishers. – 1991. – **2**. – P. 313 – 365.
8. *Scigress Explorer Ultra 7.7*, Molecular Modelling in Chemistry and Drug Design, Fujitsu Limited, Poland, 2008.
9. *Allinger N.L., Yuh Y.H., Lii J.H.* // J. Amer. Chem. Soc. – 1989. – **11**. – P. 8551 – 8566.
10. *Bowen J.P., Shim J.Y.* // J. Comp. Chem. – 1998. – **19**. – P. 1370 – 1386.
11. *Farrugia L.J.* // J. Appl. Crystallogr. – 1997. – **30**. – P. 565.
12. *Ou C.C., Powers D.A., Thich J.A. et al.* // Inorg. Chem. – 1978. – **17**. – P. 34.
13. *Dijkstra A.* // Acta Crystallogr. – 1966. – **20**. – P. 588 – 590.
14. *DeMeester P., Hodgson D.J.* // J. Amer. Chem. Soc. – 1977. – **99**. – P. 6884 – 6889.
15. *Vander Helm D., Lawson M.B., Enwall E.L.* // Acta Crystallogr., Sect. – 1971. – **B27**. – P. 2411 – 2418.
16. *Stephens F.S., Vagg R.S., Williams P.A.* // Acta Crystallogr., Sect. – 1977. – **B33**. – P. 433 – 437.
17. *Solomon E.I., Lowery M.D.* // Science. – 1993. – P. 1575.
18. *Solomon E.I.* // Inorg. Chem. – 2006. – **45**. – P. 8012 – 8025.
19. *Shoba D., Karabacak M., Periandy S. et al.* // Spectrochimica Acta Part. – 2011. – **A81**. – P. 504 – 518.
20. *Shoba D., Karabacak M., Periandy S. et al.* // Spectrochimica Acta Part. – 2011. – **A83**. – P. 540 – 552.